ISSN (Print) 1226-1750
ISSN (Online) 2233-6656
Journal of Magnetics 30(4), 615-618 (2025) https://doi.org/10.4283/JMAG.2025.30.4.615

Shape Magnetic Anisotropy Field in Permalloy Ellipses for Sensor Applications

Dae-Yun Lim and Seungha Yoon*

Energy & Nano R&D Group, Korea Institute of Industrial Technology, Gwangju 61012, Republic of Korea

(Received 29 August 2025, Received in final form 12 November 2025, Accepted 14 November 2025)

Controlling magnetic anisotropy is essential for obtaining the desired magnetic properties in functional spintronic devices. In patterned structures, the shape of the magnetic units and the fabrication conditions significantly influence magnetic switching behavior and the occurrence of ferromagnetic resonance. This study investigates the magnetic anisotropies in Permalloy ($Ni_{79}Fe_{21}$) ellipses using ferromagnetic resonance measurements and theoretical analysis. The shift in the ferromagnetic resonance peak is directly linked to variations in the effective magnetic fields within the patterned ellipses.

Keywords : magnetic anisotropy, Permalloy, shape, intrinsic, aspect ratio

1. Introduction

There is strong interest in developing advanced magnetic materials and patterning techniques [1-5]. Patterned magnetic films, in particular, have attracted significant attention due to their potential in imaging devices [6-8] and sensor applications [9-11]. The magnetization behavior of magnetic materials is governed by magnetic anisotropy, which is influenced by intrinsic factors determined during deposition and annealing, as well as by the geometry of the pattern and mechanical stresses such as bending. As a result, the combined contributions from intrinsic, shape, and stress anisotropies dictate the overall internal magnetic properties of the system.

Ferromagnetic resonance (FMR) [12, 13] serves as a key technique for probing the magnetic properties and also offers promising utility in applications, such as radar-absorbing materials, ultrafast magnetic storage, and magnetic sensing devices. FMR measures the microwave energy absorbed when a material is exposed to an effective magnetic field and electromagnetic waves at the natural precession frequency of its magnetic moments. By engineering different magnetic anisotropy from crystalline, shape, or stress in thin films and patterned structures, the resonance frequency can be precisely tuned for specific functionalities [14-17].

*Corresponding author: Tel: +82-62-600-6580
e-mail: yoonsh@kitech.re.kr

This study aimed to investigate the net magnetic anisotropy field in patterned Permalloy ($Ni_{79}Fe_{21}$) ellipses using FMR measurements and theoretical analysis. By altering the pattern shape to modify the magnetic resonance field or frequency, new opportunities can arise for developing more efficient, adaptable, and high-performance devices in flexible applications.

2. Experimental

2.1. Sample preparation

The ellipse arrays were fabricated using conventional photolithography and DC magnetron sputtering on 12 mm × 12 mm polyethylene-naphthalate (PEN) substrates. PEN substrate was selected with a good thermal stability and flexibility for further studies. During sputtering, an external magnetic field of approximately 20 mT was applied along the y-axis using permanent magnets embedded in the sample holder to induce intrinsic magnetic anisotropy along that direction. The fabricated layers included a 27 nm Permalloy layer, with 3.6 nm tantalum layers on both the top and bottom for adhesion and protection. Fig. 1(a) illustrates the geometry of the long and short axes of the patterned ellipses, along with the external DC and RF magnetic fields during ferromagnetic resonance. Figs. 1(b) and 1(c) show the fabricated ellipse arrays with aspect ratios (width along the x-axis/height along the y-axis) of 0.5 (20 μm/40 μm) and 1.0 (20 μm/20 μm), respectively.

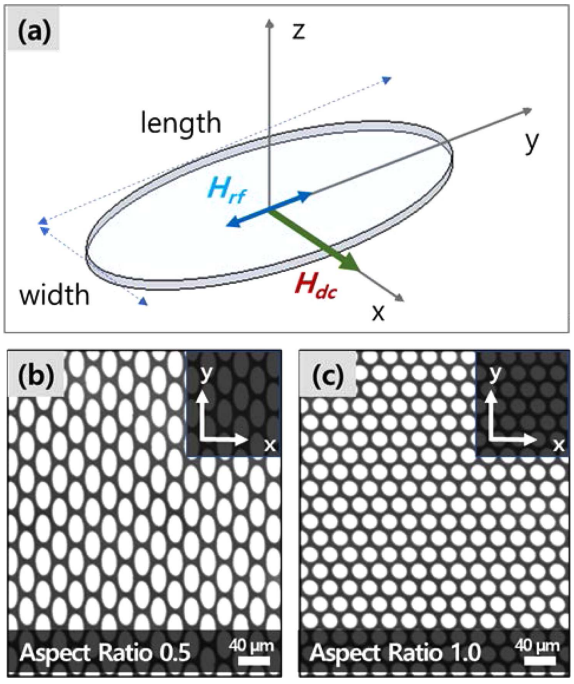

Fig. 1. (Color online) (a) illustrates the coordinates representing the length and width of the patterned ellipse, along with the applied DC and RF external magnetic fields. Figs. 1(b) and 1(c) display the patterned ellipse arrays with aspect ratios of 0.5 and 1.0, respectively.

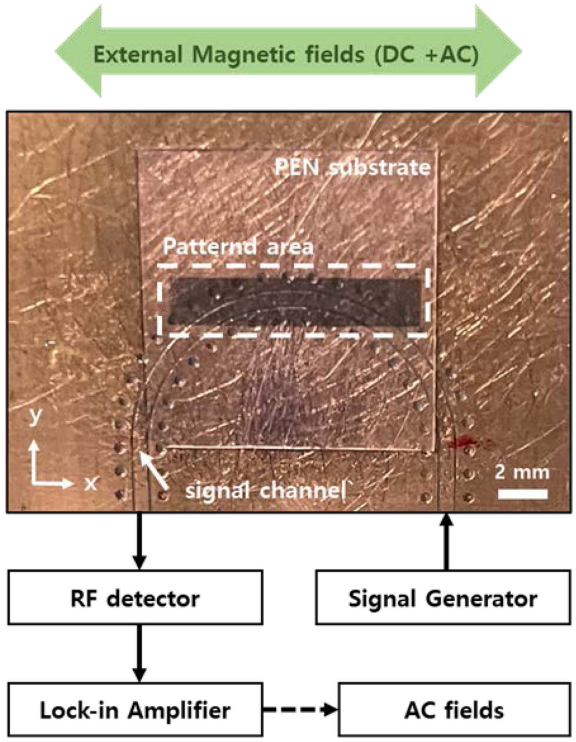

Fig. 2. (Color online) Illustrates the ferromagnetic resonance detection for elliptical arrays. The external magnetic field consists of a DC component and an AC component, generated by the pick-up coil and controlled by a reference signal of lock-in amplifier. The patterned region is located at the center of the flexible substrate and positioned face-down on the coplanar waveguide.

2.2. Measurement

The aspect ratios were chosen to systematically investigate the effect of shape anisotropy on the FMR properties of the elliptical arrays. To accurately evaluate their RF microwave absorption capabilities, the substrate was deliberately placed face down on the signal channel of a coplanar waveguide (CPW), as shown in Fig. 2(a), to enhance the interaction between the magnetization and the microwave field. In this configuration, the working frequency range was limited to 18 GHz due to the constraints of the RF cables and connectors. Nevertheless, this range is sufficient for performing FMR analyses on Permalloy thin films and patterns with applying an external magnetic field of up to 500 mT. Additionally, a vibrating sample magnetometer (VSM) was used to observe the magnetic moment as a function of the external magnetic field in specific directions. The axis coordinates representing the measurement geometry are depicted in the inset of Fig. 1. The details of the FMR detection system are illustrated in the Fig. 2(b).

2.3. Theoretical model

LL equation demonstrates the magnetization dynamics under an external magnetic field with a damping. This study applied RF magnetic field using coplanar waveguide to compensate damping. Therefore, the external DC magnetic field (H_{DC}) and RF magnetic field were applied along the x-axis and y-axis, respectively. The results of LL equation for a ferromagnetic resonance could be described by,

$$\frac{d\boldsymbol{M}}{dt} = -\gamma_e \boldsymbol{M} \times (\boldsymbol{H} + \boldsymbol{H}_{eff}) \quad (1)$$

γ_e is the electron gyromagnetic ratio, and $\boldsymbol{M}$ is the magnetization vector. $\boldsymbol{H}$ corresponds to both an external constant magnetic field ($\boldsymbol{H}_{DC}$) and RF magnetic field ($\boldsymbol{H}_{RF}$). $\boldsymbol{H}_{eff}$ is an effective magnetic field including various anisotropy fields. Under a resonance condition, the result can describe the relation between the resonance frequency and the effective magnetic fields. In particular, the contribution of the demagnetization field ($\boldsymbol{H}_D$) depending on the pattern shape was defined as NM in each axis and included in the calculation. The result of LL equation could be demonstrated as the Kittel's equation below,

$$f_{res} = \gamma_e \sqrt{(H_{DC}+H_U+M_S(-N_x+N_y))(H_{DC}+H_U+M_S(-N_x+N_z))} \quad (2)$$

f_{res} is defined as the resonance frequency. $\boldsymbol{H}_U$ is the induced anisotropy field from the deposition process. M_S is the saturation magnetization of Permalloy. The size of the ellipses could be considered as the oblate spheroid model. The demagnetization factors (N_D) are defined with r (= width (or length)/thickness),

$$N_z = \frac{4\pi r^2}{r^2-1}\left(1 - \sqrt{\frac{1}{r^2-1}}\sin^{-1}\frac{\sqrt{r^2-1}}{r}\right), \quad N_x \approx N_y = \frac{\pi^2}{r} \quad (3)$$

The calculated demagnetization factors are represented in the Fig. 3(a), when the ratio (r) varied to 100. Finally, the effective field that including the intrinsic magnetic and the shape magnetic anisotropy in the ellipse is defined as,

$$H_{eff} = \left(\frac{2K_U}{M_S} + M_S(N_x - N_y)\right)\sin(\theta) \quad (4)$$

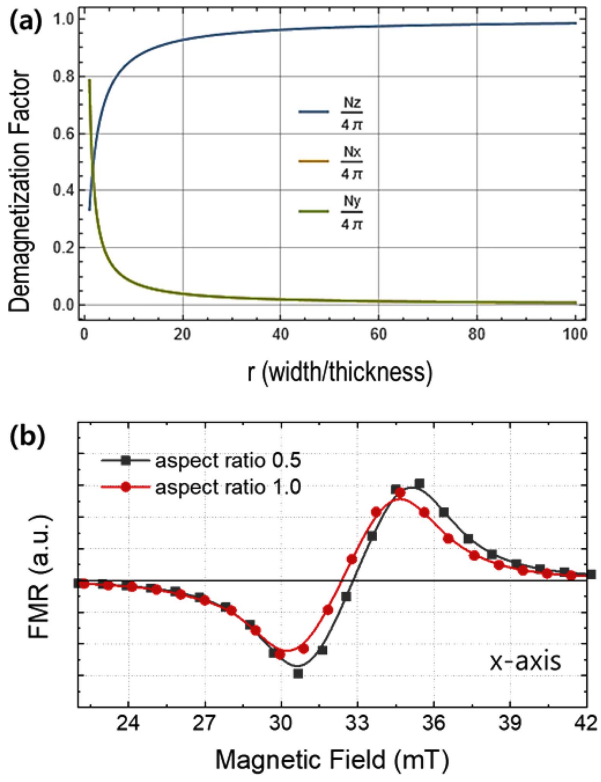

Fig. 3. (Color online) (a) shows the demagnetization factors in the spheroid oblate model as a function of the ratio between the pattern's width and thickness. (b) presents the ferromagnetic resonance curves for ellipse arrays with aspect ratios of 0.5 and 1.0.

, where K_U is induced anisotropy energy from the deposition, θ is the angle between the saturation magnetization and the deposition field direction (y-axis).

3. Results and Discussion

Figure 3(b) shows the variation in the resonance field of Permalloy ellipse arrays as a function of aspect ratio, with an external magnetic field applied along the x-axis at a constant RF of 5 GHz. The resonance field shifted from 32.9 mT to 32.3 mT, when the aspect ratio changes from 0.5 to 1.0. These consistent resonance field shifts, corresponding to changes in the shape magnetic anisotropy field, highlight the precise control over the magnetic behavior by designing pattern shapes.

The normalized magnetization curves of the ellipse arrays, detected by VSM under an external magnetic field, are shown in Fig. 4(a) and (b), with the magnetic field applied along the x-axis and y-axis, respectively. Due to the 20 mT magnetic field applied along the y-axis during sputtering (deposition field), the hysteresis loops in Fig. 4(b) show more squared curves compared to those in Fig. 4(a). Consequently, the exchange interaction between the Permalloy arrays likely induced a slightly shift of the

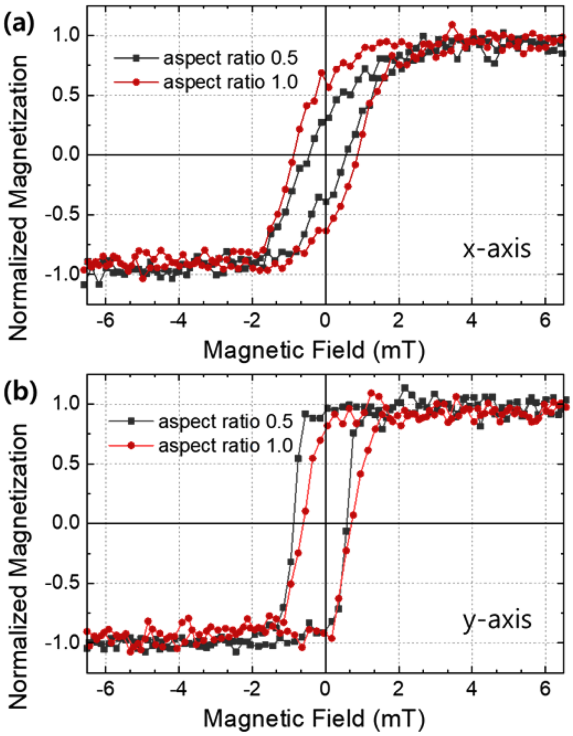

Fig. 4. (Color online) (a) and (b) show the magnetization reversal behaviors of ellipse arrays with aspect ratios of 0.5 and 1.0, in response to the external magnetic field applied along the x-axis and y-axis, respectively.

magnetization curves toward the negative field direction along the y-axis, leading to small asymmetric magnetization reversal behaviors of the Py arrays in the y-axis compared to the x-axis. Additionally, the magnetization behavior was influenced by the different aspect ratios. The squareness (remanence/saturation magnetization) of the ellipses in the x-direction was 0.25 and 0.5 for the aspect ratios of 0.5 and 1.0, respectively. In the y-direction, squareness decreased from 0.9 to 0.75 as the aspect ratio increased from 0.5 to 1.0. The saturation magnetization of the Permalloy thin film, measured by VSM, was 695.2 emu/cm³ in both the x- and y-directions. Comparing to theoretical Permalloy magnetization of around 730 emu/cm^3, the smaller magnetization was caused by the interfacial dead layers between the seed (or capping) layer and Permalloy layer.

4. Conclusion

The results clearly demonstrate that the magnetic properties of elliptical arrays can be effectively tailored through shape anisotropy. The aspect ratio on magnetic anisotropy is validated by two key observations: variations in the microwave absorption frequency and in the magnetization reversal behavior. When the external magnetic field was applied along the major y-axis of the ellipses, the squareness increased from 0.25 to 0.5 when the aspect ratio was raised from 0.5 to 1.0. In contrast, the ferromagnetic resonance field decreased slightly from 32.9 mT to 32.3 mT with increasing aspect ratio. These findings highlight the ability to precisely tune magnetic anisotropy through pattern geometry, presenting a promising strategy for improving RF-based spintronic components, such as sensors, absorbers, and antennas, by enabling enhanced control and optimization of their performance.

Acknowledgment

This study has been conducted with the support by the Korea Institute of Energy Technology Evaluation and Planning (KETEP) and the Ministry of Trade, Industry & Energy (MOTIE) of the Republic of Korea (No. RS-2024-00400653) and Korea Institute of Industrial Technology (KITECH UR-25-0103).

References

[1] H. Gleskova, S. Wagner, and D. S. Shen, IEEE Electron Device Lett. **16**, 418 (1995).
[2] P. Gruszecki, C. Banerjee, M. Mruczkiewicz, O. Hellwig, A. Barman, and M. Krawczyk, Solid State Physics **70**, 79 (2019).
[3] W.-Y. Kwak, S. Yoon, J.-H. Kwon, P. Grünberg, and B. K. Cho, J. Appl. Phys. **119**, 023904 (2016).
[4] Seungha Yoon, Youngman Jang, Chunghee Nam, J. A. Currivan, B. K. Cho, and C. A. Ross, IEEE Magn. Lett. **3**, 4000104 (2012).
[5] S. Yoon, Y. Jang, K.-J. Kim, K.-W. Moon, J. Kim, C. Nam, S.-B. Choe, and B. K. Cho, J. Appl. Phys. **111**, 07B910 (2012).
[6] H.-J. Chia, F. Guo, L. M. Belova, and R. D. McMichael, Phys. Rev. B **86**, 184406 (2012).
[7] F. Guo, L. M. Belova, and R. D. McMichael, Phys. Rev. Lett. **110**, 017601 (2013).
[8] C. A. Horwitz, W. Henle, G. Henle, H. Polesky, H. Wexler, and P. Ward, Blood **47**, 91 (1976).
[9] J.-H. Kwon, W.-Y. Kwak, and B. K. Cho, Sci. Rep. **8**, 15765 (2018).
[10] H. Zhao, R. Su, L. Teng, Q. Tian, F. Han, H. Li, Z. Cao, R. Xie, G. Li, X. Liu, and Z. Liu, Nanoscale **14**, 1653 (2022).
[11] S.-Y. Cai, C.-H. Chang, H.-I. Lin, Y.-F. Huang, W.-J. Lin, S.-Y. Lin, Y.-R. Liou, T.-L. Shen, Y.-H. Huang, P.-W. Tsao, C.-Y. Tzou, Y.-M. Liao, and Y.-F. Chen, ACS Appl. Mater. Interfaces **10**, 17393 (2018).
[12] J. R. Macdonald, Proc. Phys. Soc. Sect. A **64**, 968 (1951).
[13] S. Yoon, J. Liu, and R. D. McMichael, Phys. Rev. B **93**, 14423 (2016).
[14] S. Oyarzún, A. Tamion, F. Tournus, V. Dupuis, and M. Hillenkamp, Sci. Rep. **5**, 14749 (2015).
[15] T. Devolder, P.-H. Ducrot, J.-P. Adam, I. Barisic, N. Vernier, J.-V. Kim, B. Ockert, and D. Ravelosona, Appl. Phys. Lett. **102**, 022407 (2013).
[16] F. D. Stacey, Nature **188**, 134 (1960).
[17] C. T. Wolowiec, J. G. Ramírez, M.-H. Lee, N. Ghazikhanian, N. M. Vargas, A. C. Basaran, P. Salev, and I. K. Schuller, Phys. Rev. Mater. **6**, 064408 (2022).